

# CHEMISTRY

---

## AN ASIAN JOURNAL

www.chemasianj.org

### Accepted Article

**Title:** Selenacalix[4]dithienothiophene: Synthesis, Structure, and Complexation of A Selenide-Bridged Dithienothiophene Cyclic Tetramer

**Authors:** Masashi Hasegawa, Kazuhiro Takahashi, Ryota Inoue, Shiori Haga, and Yasuhiro Mazaki

This manuscript has been accepted after peer review and appears as an Accepted Article online prior to editing, proofing, and formal publication of the final Version of Record (VoR). This work is currently citable by using the Digital Object Identifier (DOI) given below. The VoR will be published online in Early View as soon as possible and may be different to this Accepted Article as a result of editing. Readers should obtain the VoR from the journal website shown below when it is published to ensure accuracy of information. The authors are responsible for the content of this Accepted Article.

**To be cited as:** *Chem. Asian J.* 10.1002/asia.201801105

**Link to VoR:** <http://dx.doi.org/10.1002/asia.201801105>

A Journal of



A sister journal of *Angewandte Chemie*  
and *Chemistry – A European Journal*

---

WILEY-VCH

# Selenacalix[4]dithienothiophene: Synthesis, Structure, and Complexation of A Cyclic Tetramer of Selenide-Bridging Dithienothiophene

Masashi Hasegawa\*, Kazuhiro Takahashi, Ryota Inoue, Shiori Haga, Yasuhiro Mazaki

Dedication ((optional))

**Abstract:** An efficient cyclization toward a cyclic tetramer of dithienothiophene (DTT) linked by divalent selenium atoms has been developed via palladium-catalyzed coupling reaction of  $(^n\text{Bu}_3\text{Sn})_2\text{Se}$ . X-ray analysis revealed its highly symmetrical structure having alternate arrangement of DTT units. There are several  $\text{Se}\cdots\pi$  interactions to form a supramolecular network leading to large void channel space. The cyclic tetramer possesses moderate electron-donating ability. Furthermore, the cyclic tetramer undergoes complexation with  $\text{C}_{60}$  in 1:2 ratio in the solid state to give highly symmetrical three-dimensional array of  $\text{C}_{60}$ .

In past few decades, cyclic oligothiophenes and their analogues have fascinated many chemists in various fields.<sup>[1,2]</sup> A number of two-dimensional planar oligothiophenes linked by  $\pi$ -conjugated spacers have been so far developed owing to their promising application for material science as well as their fundamental scientific interests.<sup>[3]</sup> On the contrary, the preparation of oligothiophenes has been studied to a lesser extent in three-dimensional (3D) architecture, although they can offer novel features that can not be obtained from planar structure.<sup>[4]</sup>

Thiacalix[4]thiophenes (**1**), which consist of four sets of thienylene units and sulfide linkers, are cyclic thiophene oligomers (Figure 1).<sup>[5]</sup> The combination of the aromatic subunits and divalent angular  $-\text{S}-$  bonds renders the molecular structure non-planar geometry. Recently, we reported a one-pot approach for such cyclic compounds from a simple a precursor of thiophene or dithieno[3,2-*b*:2',3'-*d'*]thiophenes (DTTs) derivatives with  $(^n\text{Bu}_3\text{Sn})_2\text{S}$ .<sup>[6,7]</sup> Palladium catalyzed coupling under Migita-Kosugi conditions<sup>[8]</sup> successfully led to the thiacalix[4]thiophene (**1**) or -DTT (**2**) in high yield, respectively. This result motivates us to synthesize 3D macrocycles linked by other heteroatoms, in particular selenium-linked cyclic compounds.

Organoselenium compounds have received considerable attention because of their potential application not only for key intermediates in organoselenium chemistry but also for building block in biologically active molecules and pharmaceuticals.<sup>[9]</sup> In addition, thanks to the large van der Waals radius of Se, supramolecular three-dimensional network can be formed in the solid state.<sup>[10]</sup> This packing force contributes to well-ordered network that can be conductive organic materials having possible hole/electron transporting properties. Therefore, selenicalix[*n*]thiophene and its derivatives are particularly

attractive because they can provide enhanced dimensionality with a large host cavity, leading to a molecular assembled porous materials.<sup>[11]</sup> However, while a wide variety of sulfur-linked macrocycles based on  $\pi$ -framework unit have been successfully prepared, there are few examples of selenium-linked macrocyclic compounds because of the lack of efficient cyclization method.<sup>[12]</sup> In 2014, Balakrishna and co-workers prepared selenacalix[*n*]thiophenes ( $n = 4-6$ ) via aromatic electrophilic substitution with  $\text{SeCl}_2$ .<sup>[12a]</sup> In that case, only electron-donating thiophene could undergo the cyclization with Se atoms. In addition, HCl was produced during the reaction, and it could be harsh conditions while the substitution reaction proceeded. With this in mind the accessibility to Se-containing cyclic compounds, we envisage that the coupling reaction of tin-selenide,  $(^n\text{Bu}_3\text{Sn})_2\text{Se}$ ,<sup>[13]</sup> and appropriate aryl-dibromide leads to the cyclic compound (**3**). In this communications, we disclose a facile cyclization reaction of a DTT derivative to give selenacalix[4]DTT under Migita-Kosugi conditions. The solid-state structure having large porous channels with large guest-accessible void space is presented. Furthermore, we found that selenacalix[4]DTT forms 1:2 complex with  $\text{C}_{60}$ .

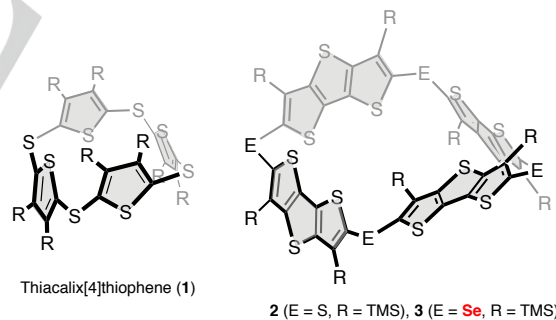


**Figure 1.** Molecular structures of thiacalix[4]thiophene and its DTT derivatives 1–3.

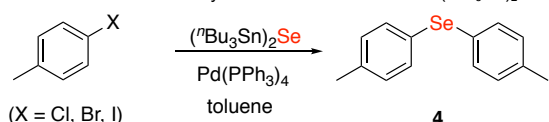
The coupling reaction to form biaryl selenides ( $\text{Ar}-\text{Se}-\text{Ar}$ ) using  $(^n\text{Bu}_3\text{Sn})_2\text{Se}$  was first developed by Nishiyama and co-workers.<sup>[14]</sup> However, they only reported the coupling of iodobenzene as the starting material in low yield. Therefore, we first optimized the reaction conditions and examined its diversity prior to the cyclization reactions (Table 1 and Figure S1). Initially, we carried out with the coupling reaction of 4-iodo-, 4-bromo-, and 4-chlorotoluene in various conditions. When 4-iodotoluene reacts with  $(^n\text{Bu}_3\text{Sn})_2\text{Se}$  in the presence of  $\text{Pd}(\text{PPh}_3)_4$  at 60 °C in toluene, compound **4** was afforded in 91 % as isolated yield (entry 1). However, compound **4** was formed in lower yield when the reaction carried out at higher temperature (entry 2). In this condition, diphenyl selenide ( $\text{Ph}_2\text{Se}$ ) and phenyl(*p*-tolyl)selenide ( $(p\text{-tol})-\text{Se}-\text{Ph}$ ) were obtained as major products, whose phenyl

[a] Dr. M. Hasegawa, K. Takahashi, R. Inoue, S. Haga, Y. Mazaki  
Department of Chemistry, Graduate School of Science  
Kitasato University, 1-15-1 Kitasato  
Minami-ku, Sagami-hara, Kanagawa 252-0373 (Japan)  
E-mail: masasi.h@kitasato-u.ac.jp

Supporting information for this article is given via a link at the end of the document.

ring(s) was/were originated from  $\text{PPh}_3$  on the catalyst. Similar exchange was occasionally found in the previous literature when the coupling reaction was carried out at higher temperature.<sup>[15]</sup> On the contrary, better yield was obtained even at higher temperature when we carried out with 4-bromotoluene (entry 4). When we applied this condition to a variety of aryl halide as the starting compounds, we obtained several biaryl selenide in good yield (80-99 %) (Figure S1).

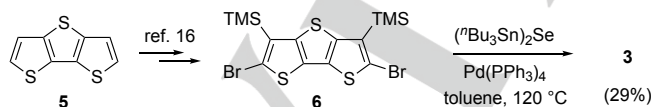
**Table 1.** Palladium-Catalyzed Reaction of Ar-X with  $(t\text{Bu}_3\text{Sn})_2\text{Se}$ <sup>[a]</sup>



Entry	X	Temp. (°C)	Time (h)	Yield (%) <sup>[b]</sup>
1	I	60	3	91
2	I	120	3	13
3	I	25	72	0
4	Br	120	3	84
5	Cl	120	72	0

<sup>[a]</sup> Conditions: *p*-tol-X (2.0 mmol),  $(t\text{Bu}_3\text{Sn})_2\text{Se}$  (1.0 mmol),  $\text{Pd}(\text{PPh}_3)_4$  (0.10 mmol), and toluene (2 mL). <sup>[b]</sup> Isolated yield.

As expected, the coupling of 2,5-dibromo-DTT derivatives **6**<sup>[16]</sup> with  $(t\text{Bu}_3\text{Sn})_2\text{Se}$  proceeded smoothly to form the cyclic products. Compound **3** was afforded in 29% yield after gel permeation chromatography (GPC) separation (Scheme 1). In sharp contrast to give various size of cyclic product in the case of  $(t\text{Bu}_3\text{Sn})_2\text{S}$  used, only cyclic tetramer together with acyclic compounds were observed. It presumably suggests that the narrower angle of C-Se-C compared to that of C-S-C disfavor to form larger cyclic products more than tetramer. Compound **3** was isolated as a stable pale yellow solid, and the molecular structure was fully characterized by ESI-MS, NMR (<sup>1</sup>H, <sup>13</sup>C, and <sup>77</sup>Se), IR, and HRMS. The formation of cyclic tetramer was confirmed by ESI-MS with a parent ion peak corresponding to  $\text{C}_{56}\text{H}_{72}\text{S}_{12}\text{Se}_4\text{Si}_8$ . The <sup>1</sup>H and <sup>13</sup>C NMR spectra revealed a highly symmetrical structure, confirming the uniformity of all DTT-Se units. The <sup>77</sup>Se NMR spectrum contains only one signal owing to the Se linkers at 346.8 ppm, exhibiting a typical chemical shift of divalent diaryl selenide.



**Scheme 1.** Synthesis of **3**

The solid-state structure was unambiguously determined by single crystal X-ray diffraction analysis (Figure 2a). The quadrilateral porous structure was obtained. The crystal was solved in the tetragonal space group  $I_4/a$ . Therefore, only a quarter unit is unique moiety. Molecules of **3** adopt a puckered quadrilateral geometry with  $S_4$  symmetry (Figure 2b), and there

exists the improper rotation axis at the center of the molecule. Four DTT rings adopt zig-zag geometry to avoid a steric repulsion of TMS groups at the neighboring unit, and thence **3** forms a 1,3-alternate geometry if compared as a selenacalix[4]arene analogue. The DTT walls in the 1,3-alternate geometry results in a large cavity, and its size is determined from the distance between S(1) and S(3) at the opposite sides to be ca. 8.6 Å.

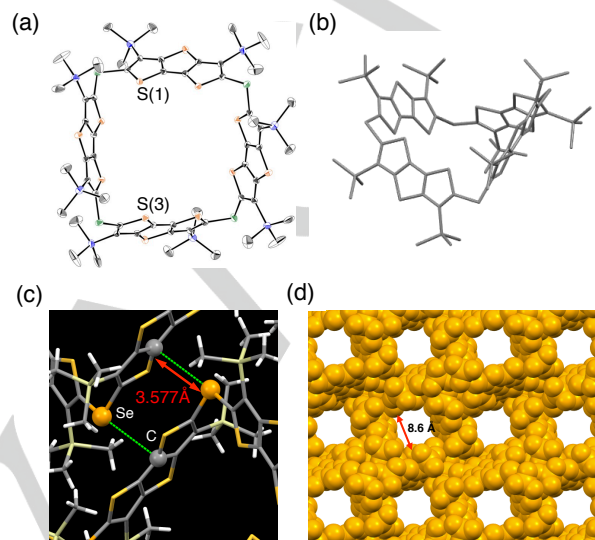


**Figure 2.** (a) ORTEP drawing of **3** with thermal ellipsoids shown at the 50% level. (b) A quadrilateral geometry of **3**. (c) Intermolecular  $\text{Se}\cdots\pi$  interactions. (d) Large void cavity in the packing diagram

In the packing diagram, a repetitive porous structure was formed through self-complementary  $\text{Se}\cdots\pi$  interactions (Figure 2c). Such a supramolecular network did not observed in other thiacalix[4]thiophene systems, and hence the incorporating of selenium atoms at the corner can reinforce the porous sheet in the crystal (Figure 2d). Some residual electron densities, which may be attributed to disordered chlorobenzene, are found in the void space between the molecules in the *c*-axis direction. The analysis of the void space suggested that the solvent-free tetragonal crystal derived from the present crystal structure has one-dimensional nano porous array with a large void volume of 2506 Å<sup>3</sup> within a unit cell (10097 Å<sup>3</sup>) (Figure 3). This porous feature implies potential application for guest-inclusion materials based on cavity-assembled porous (CAP) materials.<sup>[11]</sup>

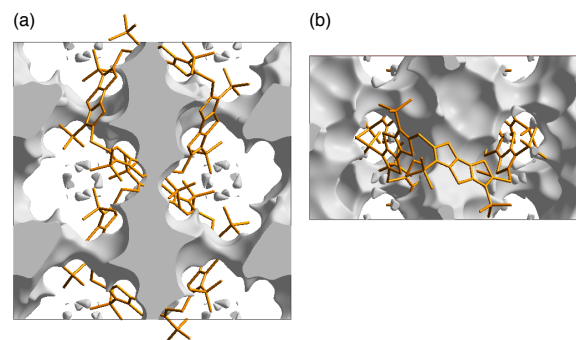


**Figure 3.** a) Crystal void channel of **3**, along the *c*-axis, and b) along the *b*-axis.

Calix[4]arenes are known to have four conformers: 1,3-alternate, 1,2-alternate, cone, and partial cone. However, present selenacalix[4]DTT has only limited conformers because of the large TMS groups at the  $\beta$  position. From density functional theory (DFT) calculations of **3**, at B3LYP/6-31G(d,p) level, 1,3-alternate geometries with  $S_4$  ( $0.00 \text{ kJmol}^{-1}$ ) and  $D_{2d}$  ( $+0.49 \text{ kJmol}^{-1}$ ) are obtained as stable conformers (Table S2).<sup>[17]</sup> The former, the most stable geometry, was a similar geometry found in the crystal structure, and it adopts a puckered to avoid steric hindrance of the TMS group. As shown in Figure 4, the HOMO exhibits large amplitudes both on the Se atoms and DTT skeleton. The lobes on the Se atoms and DTT units orthogonally interact each other. In contrast, the LUMO mainly located on DTT with quinoidal orbital topology.

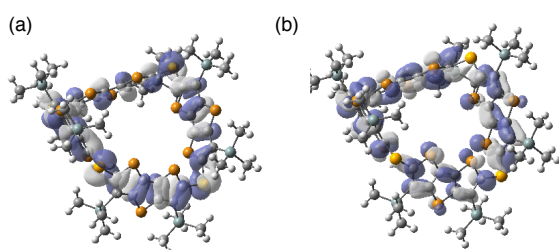


**Figure 4.** Kohn-Sham plots of the (a) HOMO and (b) LUMO of **3**.

Redox behavior of **3** was investigated by cyclic voltammetry (CV) and differential pulse voltammetry (DPV) in a 1,2-dichloroethane solution. CV of **3** revealed reversible peaks together with additional wave in higher potentials. Thus, we recorded oxidation potential from DPV experiments that reveal fine peaks. Table 1 summarized the oxidation potential obtained from DPV measurements. The first oxidation potential of **3** ( $E_{1}^{\text{ox}} = +0.51 \text{ V vs. Fc/Fc}^+$ ) is comparable to  $E_{1}^{\text{ox}}$  and  $E_{2}^{\text{ox}}$  of **2**, which are two one-electron oxidation processes, but it is much lower than **4**, which is a pristine DTT framework. Thus, the first redox was owing to  $\pi$ -conjugated selenide of Se-DTT-Se moieties. It suggests that the selenide linkers considerably enhance the electron-donating ability of the DTT subunits. This result is consistent with the electron density distribution of HOMO found in DFT calculations.

**Table 2.** Oxidation potentials of **3** and related compounds.<sup>[a]</sup>

Compound	$E_{1}^{\text{ox}}$	$E_{2}^{\text{ox}}$	$E_{3}^{\text{ox}}$
<b>3</b>	0.51	1.00	–
<b>4</b> <sup>[b]</sup>	0.90	–	–
<b>2</b> <sup>[c]</sup>	0.46 (1e <sup>-</sup> )	0.54 (1e <sup>-</sup> )	1.00

<sup>[a]</sup> Obtained by DPV measurements in  $\text{C}_2\text{H}_4\text{Cl}_2$  containing 0.1 M  $n\text{-Bu}_4\text{NPF}_6$  at 25 °C with Pt working and counter electrodes. Potentials (V) were measured against  $\text{Ag/Ag}^+$  using a luggin capillary and converted to the values vs.  $\text{Fc/Fc}^+$ . <sup>[b]</sup>  $\text{CH}_2\text{Cl}_2$  was used as a solvent. <sup>[c]</sup> Data from ref. 6.

To examine the potential ability of **3** as a receptor molecule, complexation studies with  $\text{C}_{60}$  in solution was carried out.<sup>[18]</sup> However, conventional titration experiments to determine association constant in solution were unsuccessful, because extremely insoluble materials appeared when a solution of  $\text{C}_{60}$  was added into a solution of **3**. On the other hand, very slow mixing of triple layer, composed of **3** in *o*-xylene,  $\text{C}_{60}$  in  $\text{CS}_2$ , and 1,4-dioxane as a medium layer, gave black crystals suitable for X-ray diffraction analysis.

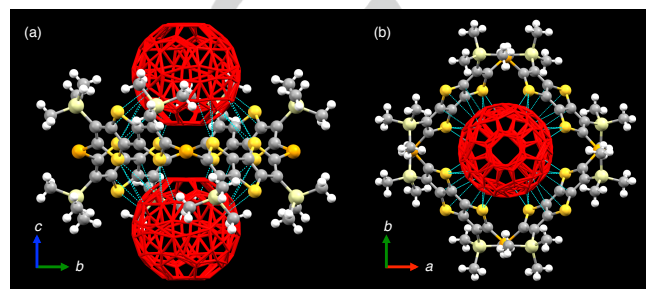


**Figure 5.** (a) and (b) Molecular structure of 1:2 complex of  $3 \cdot 2\text{C}_{60}$  obtained by X-ray analysis. Two  $\text{C}_{60}$  molecules are identical, although they are found as statically disordered in the crystal. Blue lines indicate van der Waals contacts between **3** and  $\text{C}_{60}$ .

The X-ray analysis of the solid-state structure revealed 1:2 composites of **3** and  $\text{C}_{60}$ , together with residual solvent (xylene), similar to those found in the complex of **2** with  $\text{C}_{60}$ . The complex crystallizes in the tetragonal system,  $I-4$  space group. Both two  $\text{C}_{60}$  molecules are crystallographically identical and exhibit static disorder. The diagonally located two Se atoms are separated by 14.1 Å, and the size of the host molecule is larger than  $2\text{-C}_{60}$  complex (diagonal distance of  $\text{S} \cdots \text{S}$ : 13.7 Å). There are several van der Waals,  $\pi$ - $\pi$  and sulfur- $\pi$  interactions between DTT units of **3** and  $\text{C}_{60}$ . In the crystal packing, the complex of  $3 \cdot 2\text{C}_{60}$  afforded highly symmetrical array along the axis direction. Hence,  $\text{C}_{60}$  were closely packed in the crystal.

To gain further insight into the 1:2 complex formation, the single point energy calculation were carried out at M05-2X/6-31G(d,p) level. The molecular coordinates, extracted from the geometries obtained by X-ray analysis, were employed for the calculation of the complex. In the Kohn-Sham orbital plots, the HOMO mainly locates on **3**, while the LUMO are only found in  $\text{C}_{60}$  molecules (Figure S5). The LUMO spread parallel to the nearest two DTT units. The sum of the Mulliken charges on each  $\text{C}_{60}$  molecule was small positive at +0.099 rather than negative, while those on **3** was negative at -0.198 rather than positive. Thus, the calculations demonstrate that no obvious electrostatic interactions between one  $\text{C}_{60}$  and **3** in the ground state. In fact, Raman spectroscopy does not exhibit detectable change between  $3 \cdot 2\text{C}_{60}$  and free- $\text{C}_{60}$ . Therefore, charge-transfer interactions would be a barely detectable level, if present that in the crystal. Instead, van der Waals contacts between  $\text{C}_{60}$  and two pair of DTT rings are contributed to form the complex in the solid state.

In conclusion, we have synthesized a novel Se-containing macrocycle: selenacalix[4]dithienothiophene (selenacalix[4]DTT) **3**, which is a cyclic tetramer of DTT linked with divalent Se

atoms, via one-pot Pd-catalyzed reaction. A facile coupling of dibromo DTT derivatives with  $(^n\text{Bu}_3\text{Sn})_2\text{Se}$  gave **3** in moderate yield. X-ray diffraction analysis revealed the molecular structure having non-planar quadrilateral shape with  $S_4$  symmetry, and its cavity arranged in channel-like columnar structure along the axis direction thanks to the  $\text{Se}\cdots\pi$  intermolecular interactions. The complex with two  $\text{C}_{60}$  was formed in the solid state via van der Waals interactions, and it gives symmetrical three-dimensional array of  $\text{C}_{60}$ .

## Acknowledgements

This work was supported by JSPS KAKENHI (grant nos. 20438120 and 16K17871) and research grant from Kitasato Research Center for Environment Science. The authors would like to thank Dr. Masahumi Ueda, Dr. Yasutoshi Kasahara (Kitasato University), Prof. Dr. Tohru Nishinaga (Tokyo Metropolitan University), and Dr. Hiroyasu Sato (Rigaku Co. Ltd.) for their helpful discussion. All calculations were performed at the Research Center for Computational Science, Okazaki (Japan).

**Keywords:** calix[n]arene • selenium • coupling reaction •  $\text{C}_{60}$  complex • large void space

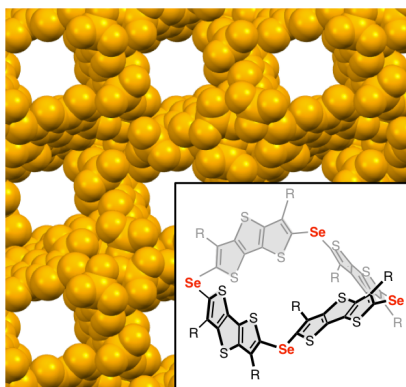
- [1] a) M. Iyoda, H. Shimizu, *Chem. Soc. Rev.* **2015**, *44*, 6411–6424; b) M. E. Cinar, T. Ozturk, *Chem. Rev.* **2015**, *115*, 3036–3140; c) L. Zhang, N. S. Colella, B. P. Cherniawski, S. C. B. Mannsfeld, A. L. Briseno, *ACS Appl. Mater. Interfaces*, **2014**, *6*, 5327–5343; d) A. Mishra, C.-Q. Ma, P. Bäuerle, *Chem. Rev.* **2009**, *109*, 1141–1276.
- [2] I. F. Perepichka, D. F. Perepichka Eds., *Handbook of Thiophene-based Materials: Applications in Organic Electronics and Photonics*, Wiley-VCH: Chichester, U.K., 2009.
- [3] For selected examples, see: a) M. Iyoda, K. Tanaka, H. Shimizu, M. Hasegawa, T. Nishinaga, T. Nishiuchi, Y. Kunugi, T. Ishida, H. Otani, H. Sato, K. Inukai, K. Tahara, Y. Tobe, *J. Am. Chem. Soc.* **2014**, *136*, 2389–2396; b) F. Zhang, G. Götz, E. Mena-Osteritz, M. Weil, B. Sarkar, W. Kaim, P. Bäuerle, *Chem. Sci.* **2011**, *2*, 781–784; c) T. Takahashi, K.-i. Matsuoka, K. Takamiya, T. Otsubo, Y. Aso, *J. Am. Chem. Soc.* **2014**, *127*, 8928–8929; d) T. Nishinaga, S. Shiroma, M. Hasegawa, *Org. Lett.* **2018**, *20*, 3426–3429.
- [4] For recent examples, see: a) M. Hasegawa, K. Kobayakawa, H. Matsuzawa, T. Nishinaga, T. Hirose, K. Sako, Y. Mazaki, *Chem. Eur. J.* **2017**, *23*, 3267–3271; b) H. Ito, Y. Mitamura, Y. Segawa, K. Itami, *Angew. Chem., Int. Ed.* **2015**, *54*, 159–163; *Angew. Chem.* **2015**, *127*, 161–165; c) F. Sannicoló, P. R. Mussini, T. Benincori, R. Cirilli, S. Abbate, S. Arnaboldi, S. Casolo, E. Castiglioni, G. Longhi, R. Martinazzo, M. Panigati, M. Pappini, E. Q. Procopio, S. Rizzo, *Chem. Eur. J.* **2014**, *20*, 15298–15302; d) W. Gao, J. Wang, Q. Luo, Y. Lin, Y. Ma, J. Dou, H. Tan, C.-Q. Ma, Z. Cui, *RSC Adv.* **2017**, *7*, 1606–1616.
- [5] a) B. König, M. Rödel, I. Dix, P. G. J. Jones, *Chem. Res., Synop.* **1997**, 69; b) J. Nakayama, N. Katano, Y. Sugihara, A. Ishii, *Chem. Lett.* **1997**, 897; c) N. Katano, Y. Sugihara, A. Ishii, J. Nakayama, *Bull. Chem. Soc. Jpn.* **1998**, *71*, 2695–2700.
- [6] R. Inoue, M. Hasegawa, T. Nishinaga, K. Yoza, Y. Mazaki, *Angew. Chem. Int. Ed.*, **2015**, *54*, 2734–2738; *Angew. Chem.* **2015**, *127*, 2772–2776.
- [7] a) M. Hasegawa, R. Inoue, Y. Mazaki, *Synlett*, **2016**, 27, 2407–2415; b) M. Hasegawa, Y. Honda, R. Inoue, Y. Mazaki, *Chem. Asian J.* **2016**, *11*, 674–677.
- [8] a) M. Kosugi, K. Shimizu, A. Ohtani, T. Migita, *Chem. Lett.* **1981**, 829–830; b) M. Kosugi, T. Ogata, M. Terada, H. Sano, T. Migita, *Bull. Chem. Soc. Jpn.* **1985**, *58*, 3657–3658.
- [9] a) C. W. Nogueira, G. Zeni, J. B. T. Rocha, *Chem. Rev.* **2004**, *104*, 6255–6286; (b) S. T. Manjare, Y. Kim, Y.; D. G. Churchill, *Acc. Chem. Res.* **2014**, *47*, 2985–2998.
- [10] a) D. Jerome, A. Mazaud, M. Ribault, K. Bechugaard, *Phys. Lett.*, **1980**, *41*, 95–98; b) T. Izawa, E. Miyazaki, K. Takimiya, *Chem. Mater.* **2009**, *21*, 903–912; c) M. Nakano, K. Niimi, E. Miyazaki, I. Osaka, K. Takimiya, *J. Org. Chem.* **2012**, *77*, 8099–8111.
- [11] S. Tashiro, M. Shionoya, *Bull. Chem. Soc. Jpn.* **2014**, *87*, 643–654.
- [12] a) P. Kumar, V. S. Kashid, J. T. Mague, M. S. Balakrishna, *Tetrahedron Lett.* **2014**, *55*, 5232–5235; b) J. Thomas, W. Maes, K. Robeyns, M. Ovaere, L. V. Meervelt, M. Smet, W. Dehaen, *Org. Lett.* **2009**, *11*, 3040–3043; c) R. H. Mitchell, *Tetrahedron Lett.* **1975**, *16*, 1363–1364.
- [13] H. Maeda, M. Takashima, K. Sakata, T. Watanabe, M. Honda, M. Segi, *Tetrahedron Lett.* **2011**, *52*, 415–417.
- [14] Y. Nishiyama, K. Tokunaga, N. Sonoda, *Org. Lett.* **1999**, *1*, 1725–1727.
- [15] F. E. Goodson, T. I. Wallow, B. M. Novak, *J. Am. Chem. Soc.* **1997**, *119*, 12441–12453.
- [16] J. Frey, A. D. Bond, A. B. Holmes, *Chem. Commun.* **2002**, 2424–2425.
- [17] Gaussian 16, Revision B.01, M. J. Frisch, G. W. Trucks, H. B. Schlegel, G. E. Scuseria, M. A. Robb, J. R. Cheeseman, G. Scalmani, V. Barone, G. A. Petersson, H. Nakatsuji, X. Li, M. Caricato, A. V. Marenich, J. Bloino, B. G. Janesko, R. Gomperts, B. Mennucci, H. P. Hratchian, J. V. Ortiz, A. F. Izmaylov, J. L. Sonnenberg, D. Williams-Young, F. Ding, F. Lipparini, F. Egidi, J. Goings, B. Peng, A. Petrone, T. Henderson, D. Ranasinghe, V. G. Zakrzewski, J. Gao, N. Rega, G. Zheng, W. Liang, M. Hada, M. Ehara, K. Toyota, R. Fukuda, J. Hasegawa, M. Ishida, T. Nakajima, Y. Honda, O. Kitao, H. Nakai, T. Vreven, K. Throssell, J. A. Montgomery, Jr., J. E. Peralta, F. Ogliaro, M. J. Bearpark, J. J. Heyd, E. N. Brothers, K. N. Kudin, V. N. Staroverov, T. A. Keith, R. Kobayashi, J. Normand, K. Raghavachari, A. P. Rendell, J. C. Burant, S. S. Iyengar, J. Tomasi, M. Cossi, J. M. Millam, M. Klene, C. Adamo, R. Cammi, J. W. Ochterski, R. L. Martin, K. Morokuma, O. Farkas, J. B. Foresman, and D. J. Fox, Gaussian, Inc., Wallingford CT, 2016.
- [18] For recent examples of  $\text{C}_{60}$  complex with  $\pi$ -conjugated macrocycle, see: a) Y. Yamamoto, E. Tsurumaki, K. Wakamatsu, S. Toyota, *Angew. Chem. Int. Ed.*, **2018**, *57*, 8199–8202; b) H. Shimizu, C. J. Jose, M. Hasegawa, T. Nishinaga, T. Haque, M. Takase, H. Otani, J. Rabe, M. Iyoda, *J. Am. Chem. Soc.*, **2015**, *137*, 3877–3885; c) K. Yoshida, A. Osuka, *Chem. Eur. J.*, **2016**, *22*, 9396–9403; d) E. Mena-Osteritz, P. Bäuerle, *Adv. Mater.* **2006**, *18*, 447–451.

Entry for the Table of Contents (Please choose one layout)

Layout 1:

## COMMUNICATION

An efficient cyclization to selenacalix[4]dithienothiophene has been developed. X-ray analysis revealed there are intermolecular  $\text{Se}\cdots\pi$  interactions to form a supramolecular network, leading to large void channel space. Furthermore, the cyclic compound forms 1:2 complex with  $\text{C}_{60}$ .



Masashi Hasegawa\*, Kazuhiro Takahashi, Ryota Inoue, Shiori Haga, Yasuhiro Mazaki

Page No. – Page No.

**Selenacalix[4]dithienothiophene: Synthesis, Structure, and Complexation of A Cyclic Tetramer of Selenide-Bridging Dithienothiophene**